

ON IONIZATION EFFECTS AND ABUNDANCE RATIOS IN DAMPED Ly α SYSTEMS

Yuri I. Izotov

*Main Astronomical Observatory, Ukrainian National Academy of Sciences, Golosiiv, Kyiv 03680, Ukraine
Electronic mail: izotov@mao.kiev.ua*

Daniel Schaerer and Corinne Charbonnel

*Laboratoire d'Astrophysique, CNRS UMR 5572, Observatoire Midi-Pyrénées, 14, Av. E. Belin, F-31400
Toulouse, France
Electronic mail: schaeerer@ast.obs-mip.fr, corinne.charbonnel@ast.obs-mip.fr*

ABSTRACT

The similarity between observed velocity structures of Al III and singly ionized species in damped Ly α systems (DLAs) suggests the presence of ionized gas in the regions where most metal absorption lines are formed. A simplified model consisting of *Region 1*) a plane-parallel ionization bounded region illuminated by an internal radiation field, and *Region 2*) a neutral region with a negligible metal content is considered. We calculate photoionization equilibrium models for region 1, and constrain the ionization parameter by the observed $N(\text{Al III})/N(\text{Si II})$ column density ratio. Under these conditions we find that ionization effects are important.

If these effects are taken into account, the element abundance ratios in DLAs are quite consistent with those observed in Milky Way stars and in H II regions of local low-metallicity blue compact dwarf galaxies. In particular we cannot exclude the same primary N origin in both DLAs and metal-poor galaxies. No depletion of heavy elements on dust grains needs to be invoked, although our models do not exclude the presence of little depletion.

Although highly simplified and relying on the strong assumption of a significantly lower metal content in region 2, our model appears to be supported by recent data on a local DLA and it is not in contradiction with the current knowledge on high redshift DLAs. If correct, it offers a clear simplification in the understanding of heavy element abundance ratios in DLAs and their comparison with the local Universe.

Subject headings: galaxies: abundances — intergalactic medium — quasars: absorption lines

Accepted for publication in ApJ

1. INTRODUCTION

Damped Lyman α systems (DLAs) are the class of QSO absorption systems showing the largest column density, with $N(\text{H I}) \gtrsim 2 \times 10^{20} \text{ cm}^{-2}$. They are considered to be the high-redshift progenitors of present-day luminous galaxies (e.g. Wolfe 1990) and dominate the neutral gas content of the Universe (Wolfe et al. 1995), a mass comparable with that of the stars in present day spiral galaxies. This may suggest that DLAs are the source of most of material available for star formation at high redshift (Lanzetta et al. 1995). Later studies have shown that probable optical counterparts of damped Ly α systems at $z \lesssim 1$ are galaxies of different morphological types (Le Brun et al. 1997).

Understanding the chemical evolutionary history of galaxies is fundamental to the study of galaxy formation. Pettini et al. (1994, 1997) have performed extensive studies on the metallicity of the damped Ly α systems at high redshift. Their results indicate a mean metallicity $\text{Zn}/\text{H} \approx 1/10$ of the solar abundance with a large dispersion. It was also noted that the element Cr is generally less abundant than Zn relative to their solar proportion. Since Zn and Cr are thought to be made in solar proportions throughout the Milky Way based on their abundances in Galactic disk and halo stars, the overabundance of Zn to Cr found in damped Ly α systems was taken as evidence that some Cr was depleted from the gas phase by dust grains.

The HIRES W.M.Keck telescope observations have opened the opportunity to study Ly α absorption lines for a large number of elements including N, O, Mg, Al, Si, S, Cr, Mn, Fe, Ni and Zn. Lu et al. (1996a), Prochaska & Wolfe (1999), Outram et al. (1999) and Pettini et al. (2000) have found that the relative abundance patterns indicate that the bulk of heavy elements in these high-redshift galaxies was produced by Type II supernovae; there is little evidence for significant contribution from low- to intermediate-mass stars or from Type Ia supernovae.

However, the current interpretation combining the effects of dust depletion and Type II supernovae enrichment (Lu et al. 1996a; Prochaska & Wolfe 1999; Vladilo 1998) leads to several inconsistencies. In this picture the overabundance of Zn relative to Cr or Fe found in DLAs is attributed to selective depletion of Cr and Fe by dust grains. However, it then turns out that such an interpretation is inconsistent with some of the other elemental abundance ratios seen in these

galaxies, in particular N/O, S/Fe, Mn/Fe and Ti/Fe. This led Lu et al. (1996a) and Prochaska & Wolfe (1999) to conclude that the overabundance of Zn relative to Cr in damped Ly α galaxies may be intrinsic to their stellar nucleosynthesis. They emphasize the need for another physical process to explain the damped Ly α abundance patterns.

Furthermore, comparisons of the distribution of Fe/H versus redshift (Lu et al. 1996a; Prochaska & Wolfe 2000) for the sample of damped Ly α galaxies with the corresponding relation for the Milky Way disk indicate that the damped Ly α galaxies are much less metal-enriched than the Galactic disk in its past. Since there is evidence that depletion of Fe by dust grains is relatively unimportant, the difference in the enrichment level between the sample of damped Ly α galaxies and Milky Way disk suggests that DLAs are probably not high-redshift spiral disks. A similar conclusion has been reached by Pettini et al. (1999). They argue that the relative abundances of heavy elements in DLA systems are consistent with a moderate degree of dust depletion that, once accounted for, leaves no room for the enhancement of α elements over iron seen in metal-poor stars in the Milky Way. Recently Centuri3n et al. (2000) have found the S/Zn abundance ratio in the relatively high-metallicity DLAs to be lower than solar ratio. This is contrary to previous assertions that DLAs have been enriched solely by Type II supernovae, but it can be understood if star formation in these systems proceeded at a lower rate than in the early history of our Galaxy (Pettini et al. 1999; Centuri3n et al. 2000).

It is generally believed that the gas in DLAs is mostly in the neutral stage due to the very high optical depth beyond the hydrogen ionization limit (e.g., Viegas 1994; Prochaska & Wolfe 1996). Therefore, it is assumed that all species with ionization potentials lower than hydrogen are in a singly ionized stage, while other species are neutral. With this assumption correction factors for ionization are small and the ratios of column densities of ions are equal to the ratios of element abundances. However, Lu et al. (1996a), Prochaska & Wolfe (1999) and Wolfe & Prochaska (2000) find a good correlation between the velocity structure of Al III and singly ionized species. The ionization potential of Al^+ is 18.8 eV, i.e. greater than that of hydrogen. Therefore, Al^{+2} is likely present in ionized, not in neutral gas. To explain the similarity of Al III and other low ionization species line profiles, Howk & Sembach (1999) and Izotov & Thuan (1999)

proposed that these lines originate in the same ionized region or in a mix of neutral and ionized clouds, and stressed the importance of abundance correction for ionization effects. Indirect arguments to consider ionized gas in DLAs come from studies of the warm ionized medium in the Milky Way and other nearby galaxies (Howk & Sembach 1999; Howk, Savage & Fabian 1999; Sembach et al. 2000; Jenkins et al. 2000).

Higher ionization species of C IV and Si IV are also observed in the spectra of DLAs. However, in the majority of cases, the C IV and Si IV profiles differ from those of lower ionization species; few cases exist where some components of the C IV and Si IV absorption lines coincide with e.g. Si II, Al II and Al III (see e.g., Lu et al. 1996a; Prochaska & Wolfe 1999; Wolfe & Prochaska 2000). The high ionization species are thus apparently formed in regions with different conditions and will not be considered here. In rare cases absorption lines from neutral species with ionization potentials below that of hydrogen, such as C I and Mg I, are observed in DLAs. The existence of such lines is a priori not in contradiction with the presence of Al III, since neutral species can also be present in small quantities in ionized gas (cf. Sect. 3).

Motivated by the close similarity between the velocity structures of Al III and singly ionized species in DLAs, which suggests the presence of ionized gas in the regions where these absorption lines are formed, we here consider a simple model that takes these effects to first order into account. We examine a model of DLAs in which absorption lines of neutral and low-ionization heavy element species originate in ionized rather than in neutral gas, and we explore the possible implications on abundance determinations in such systems. As indicated by the presence of high ionization species and the complex structure of the absorption line profiles seen in the high resolution spectra, the conditions of the absorbing gas must in reality be highly variable and of complex nature (see e.g. Lauroesch et al. 1996). In the future, both more advanced analysis of the detailed line profiles and sub-components as well as more sophisticated models allowing for complex geometries, various ISM phases etc. will be necessary to obtain a more accurate description of the absorbing systems. It is the hope that the present simplified model reflects the main trends due to ionization effects.

The model assumptions are described in Section 2. The results from the model calculations and the impli-

cations on heavy element abundance ratios in DLAs are discussed in Section 3. In Section 4 we briefly consider the application of our model to other objects and summarise the main results from this work.

2. MODELS

The above discussion shows that the properties of the damped Ly α systems are yet poorly understood. While a significant amount of neutral gas is observed in these systems, it is not clear how the regions of ionized gas are related to those of neutral gas. What is the main source of ionization in DLAs - internal stellar radiation or harder background intergalactic radiation? Where are absorption lines of heavy elements formed - in ionized or neutral gas? Is the metallicity of ionized and neutral gas similar or not? Is heavy element depletion by dust grains important?

In the present paper we explore the following “multi-component” picture for DLA systems: 1) an ionization bounded region illuminated by an internal radiation field complemented by 2) a neutral region with a lower metal content. These working hypotheses are adopted to study the main effects intrinsic stellar ionizing radiation may have on observed heavy element patterns in such conditions.

To explore the consequences of such a models we use the CLOUDY ionization equilibrium code (version c90.05; Ferland 1996; Ferland et al. 1998) to calculate the ionization state of region 1. For simplicity, we assume internal stellar radiation and consider a plane-parallel geometry. The outer boundary of the slab is determined by the condition that a low electron temperature of 2000 K is reached. For the cases discussed here (low metallicity and low dust content) this boundary condition is a good approximation for the outer boundary of ionization-bounded H II regions. For the ionizing spectrum, we adopt the spectrum of a typical O star. We use an ATLAS line-blanketed model atmosphere (Kurucz 1991) with effective temperatures $T_{\text{eff}} = 33000$ K, 40000 K and 45000K and $\log g = 4.0$. The lower temperature is likely more appropriate for the conditions in the interstellar medium of metal-rich spiral galaxies and the local ISM in our Galaxy (cf. Sembach et al. 2000). In low-metallicity environments the temperature of the ionizing radiation tend to be higher as evidenced from studies of nearby extragalactic giant H II regions (e.g. Stasińska & Leitherer 1996). The ionization parameter which is proportional to the ratio of the number density of

the ionizing photons to that of the electrons is varied in the range $U = 10^{-5} - 10^{-2}$. We consider the metal abundance of 0.1 solar, with relative element abundances equivalent to those observed in the low-metallicity BCDs (e.g., Izotov & Thuan 1999). In particular, C/O and N/O abundance ratios are reduced by factors of 2 and 5 respectively as compared to solar abundance ratios. We also adopt for ${}^4\text{He}$ the mass fraction $Y = 0.252$ (or $\log \text{He}/\text{H} = -1.07$), which is higher than the primordial mass fraction $Y_p = 0.245$ (Izotov et al. 1999), but is typical for the BCDs with the heavy element abundance 1/10 solar (Izotov & Thuan 1998). Dust grains with a dust-to-gas ratio of 1/10 that in Milky Way are taken into account in heating and cooling processes, although the differences in ionic fractions derived in the models with and without dust grains are small.

A similar model has recently been considered by Howk & Sembach (1999). The major difference with their approach is that they consider ionized density-bounded regions surrounding the neutral, H I-bearing clouds. The boundary of the ionized region is defined where the local fraction of neutral hydrogen climbs above 10%. With these assumptions the fraction of neutral species like O^0 , N^0 or Ar^0 is significantly reduced because they always reside near the edges of H II region. Additionally, the variation of the local ionization fraction of neutral hydrogen at the edge of ionized density-bounded region results in large variations of some low-ionization species, in particular, of Cr^+ and Fe^+ . Further resulting differences between the model by Howk & Sembach (1999) and our ionization-bounded model will be discussed below.

An important feature of both models is that the heavy element abundances in the ionized and neutral regions are a priori unrelated. This implies in particular that relative abundance determinations with respect to hydrogen, as derived from the observed column densities, may not be meaningful or are at least uncertain.

3. RESULTS

3.1. Ionization fractions of elements

In Table 1 we show the ionization potentials and the ionization fractions x^i of the most important ions

¹By definition the ionization fraction $x(\text{X}^{+i})$ is the ratio of the radially integrated number density of ion X^{+i} to the radially integrated total number density of the element X in all ioniza-

tion stages, i.e. $x(\text{X}^{+i}) = \int n(\text{X}^{+i})dr / \int n(\text{X})dr$, the relative column density of the ion X^{+i} .

which are observed or can potentially be observed in DLAs, as a function of the ionization parameter U for two temperatures $T_{\text{eff}} = 33000$ K and 40000 K of ionizing radiation and the heavy element mass fraction $Z = 0.1Z_{\odot}$. On the first line we also show $N(\text{H}^0 + \text{H}^+)$, the total hydrogen column density across the ionized slab. Over the entire range of U , except for the highest value shown here ($U = 10^{-2}$), $N(\text{H}^0 + \text{H}^+)$ remains significantly smaller than the column density of neutral hydrogen observed in damped Ly α system². For an ionization parameter $U \sim 10^{-5}$ hydrogen is essentially neutral, while at $U \gtrsim 10^{-3}$ it is almostly ionized as it is evidenced by small neutral hydrogen fraction $x(\text{H}^0)$ (Table 1). Calculations for lower heavy element abundances show that the ionization fractions are not strongly changed. Therefore, the data from Table 1 can be used for objects with metallicity $[\text{Fe}/\text{H}] \lesssim -1$.

The distribution of the ionic fractions $x(\text{X}^i)$ of selected ions as a function of ionization parameter U is shown in Figure 1. While the ionization fractions of all neutral and singly ionized species decrease with increasing ionization parameter U , the ionization fraction of Al^{+2} is increased. Therefore, the ratio $x(\text{Al}^{+2})/x(\text{Al}^+) = N(\text{Al III}) / N(\text{Al II})$ is a very sensitive indicator of ionization conditions and can be used to determine U . Unfortunately, although line profiles of Al II and Al III in damped Ly α systems are essentially similar (Lu et al. 1996a; Prochaska & Wolfe 1999), in the many cases the Al II lines are saturated or marginally saturated. This circumstance complicates direct estimates of the ionization parameter U . However, very often, unsaturated lines of Si II, Fe II and Al III are observed in the same spectra and they can be used to estimate U . For this, we assume that the observed heavy element abundance patterns at low metallicities are similar to that observed in low-metallicity halo stars, i.e. $[\text{Si}/\text{Fe}] \sim 0.3$, $[\text{Al}/\text{Fe}] \sim -0.4$ (Timmes et al. 1995; Samland 1998), and adopt that $\log (\text{Al}/\text{Si})_{\odot} \approx \log (\text{Al}/\text{Fe})_{\odot} \approx -1.0$ (Anders & Grevesse 1989). Then, the expected ratio of column densities is equal to

$$\log \frac{N(\text{Al III})}{N(\text{Si II})} \sim -1.7 + \log \frac{x(\text{Al}^{+2})}{x(\text{Si}^+)}, \quad (1)$$

²For $T_{\text{eff}} = 40000$ K and the ‘‘typical’’ value of $\log U \sim -3.25$ the column density is ~ 40 % of the lower limit which defines damped systems. The baryonic mass of low column density DLAs could thus be underestimated by up to this amount.

$$\log \frac{N(\text{Al III})}{N(\text{Fe II})} \sim -1.4 + \log \frac{x(\text{Al}^{+2})}{x(\text{Fe}^{+})}. \quad (2)$$

The typical values of $\log [N(\text{Al III})/N(\text{Si II})]$ and $\log [N(\text{Al III})/N(\text{Fe II})]$ in damped Ly α systems are ~ -2.0 to -2.5 and ~ -1.5 to -2.0 , respectively, which translates to $\log [x(\text{Al}^{+2})/x(\text{Si}^{+})] \sim -0.3$ to -0.8 , $[x(\text{Al}^{+2})/x(\text{Fe}^{+})] \sim -0.1$ to -0.6 , or $\log U \sim -3$ (Fig. 1). This estimated value of ionization parameter is dependent on the uncertainties in abundance determination and those for the adopted photoionized model and possible depletion of elements into grains. In principle, other single ionized species, e.g. Zn II, can be used instead of Si II or Fe II. However, Si II and Fe II absorption features are more often seen and measured in the DLAs, and the atomic data for these ions are known with better precision (Howk & Sembach 1999). The above estimate of U is based on the assumption that heavy elements are not present in the neutral gas surrounding the region of ionized gas. If the neutral gas is significantly enriched in heavy elements then an additional contribution to the column densities of Si II and Fe II comes from neutral gas and the ionization parameter should be increased to account for observed $N(\text{Al III})/N(\text{Si II})$ and $N(\text{Al III})/N(\text{Fe II})$ ratios.

Before we proceed to discuss the implications of this model when applied to observations of damped Ly α systems it is useful to recall that some neutral species with ionization potentials below that of hydrogen can be present in ionized gas as well. For instance Lu et al. (1996a) have measured $\log N(\text{Mg II}) > 14.38$ and $\log N(\text{Mg I}) = 12.44 \pm 0.04$ in the $z_{\text{damp}} = 0.8598$ system toward Q0454+0356 which are consistent with the predictions of our simplified models (Table 1). Their measurements for another $z_{\text{damp}} = 1.2667$ system toward Q0449-1326 provide only lower limits $\log N(\text{Mg II}) > 14.1$ and $\log N(\text{Mg I}) > 12.62$, also not in contradiction with the ionization model. Prochaska & Wolfe (1999) have derived $\log N(\text{C II}) > 14.6$ and $\log N(\text{C I}) < 12.8$ in the $z_{\text{damp}} = 2.140$ toward Q0149+33 which are consistent with predictions of ionization models. Hence, the presence of species like C I or Mg I does not necessarily mean that they reside in neutral gas.

A useful validity check of our model is the comparison of the predictions of photoionization models with the observed values of $[\text{O I}/\text{Si II}]$. In the case of the neutral gas model it is expected that $[\text{O I}/\text{Si II}] \sim 0$, while in the case of our ionization models $[\text{O I}/\text{Si II}] = -0.5$ - -0.8 depending on T_{eff} and for the range log

$U = -3.5$ - -3.0 (Table 1). In the majority of cases observations of DLA systems give only lower limits of O I abundance because of saturation of the O I $\lambda 1302$ absorption line. The available data in the literature shows that, in general, the lower limits of $[\text{O I}/\text{Si II}]$ are consistent with values expected from the ionization models. However, in some DLAs the lower limits of $[\text{O I}/\text{Si II}]$ are larger than those expected from the ionization models. Lu et al. (1996b) find $[\text{O I}/\text{Si II}] > -0.27$ for the $z = 4.38$ absorber towards 1202-0275, while Prochaska & Wolfe (1999) find $[\text{O I}/\text{Si II}] = -0.17$ in the absorber towards Q0951-04. These values seems difficult to reconcile with ionization models unless a low ionization parameter is appropriate. However, no measurements of Al III have been done for these absorbers which would allow to constrain the ionization parameter U .

Recently Molaro et al. (2000) have derived a high value of $[\text{O I}/\text{Si II}] = 0.0$ - 0.1 from the unsaturated O I and Si II lines in the $z = 3.39$ absorber towards the QSO 0000-2620. For this absorber $N(\text{Al III}) / N(\text{Si II}) = -2.4$ is rather high, suggesting an ionization parameter $\log U \sim -3.0$ to -3.5 . However, inspection of Fig. 1 in Prochaska & Wolfe (1999) indicates different profiles of Si II $\lambda 1808$ and Al III $\lambda 1854$ in this absorber, at variance with other absorbers rendering the estimate of the ionization parameter U rather uncertain.

The above discussion suggests that large ionized regions and abundance discontinuities might be present in some DLAs, while other DLAs might be essentially neutral. It is likely that DLAs may represent a mixed bag of systems with varying ionization conditions. While the ionization model does not pretend to explain abundance pattern in all damped Ly α systems, we conclude that in many cases the derived lower limits of $[\text{O I}/\text{Si II}]$ do not rule out this model. However, we point out that better determinations of $[\text{O I}/\text{H I}]$ are needed to test the importance of the ionization effects in the damped Ly α systems.

3.2. Age-metallicity relation and the large spread in $[\text{Fe}/\text{H}]$

A very extensive literature exists on the interpretation of the metallicity of DLA as a function of redshift (e.g. Pettini et al. 1994; Lu et al. 1996a; Lindner, Fritze - von Alvensleben & Fricke 1999; Prantzos & Boissier 2000). Among the main issues discussed are the question of apparent evolution or non-evolution of metallicity with z , the origin of the scatter, and

possible observational biases affecting this relation. A detailed comparison with such studies is beyond the scope of the present paper. Here, we shall only indicate the typical metallicity shift expected in the framework of our model and mention the main implication in terms of age-metallicity relations.

Pettini et al. (1994, 1999), Lu et al. (1996a), Prochaska & Wolfe (2000) noted that the chemical enrichment processes in damped Ly α galaxies appear to be quite inhomogeneous. The [Zn/H] and [Fe/H] distributions show a scatter by a factor of ~ 20 with the mean value of [Zn/H] which is 0.4 larger than that of [Fe/H] for the DLAs at $z \approx 2$ (Prochaska & Wolfe 2000). Furthermore, Lu et al. (1996a) and Pettini et al. (1999) noted that the degree of chemical enrichment in the sample of damped Ly α galaxies is, on average, considerably lower than the Milky Way disk at any given time in the past. This led them to conclude that the chemical enrichment of damped Ly α galaxies is different from that in the disk of Milky Way.

A possible explanation for the difference in chemical enrichment is simply that DLAs are in general not necessarily spiral galaxies (Le Brun et al. 1997). Alternatively, if in the framework of our model the heavy element lines are produced only in the ionized region (i.e. the neutral gas has a very low metal content), the real Fe/H abundance in the ionized gas is several times higher than that derived from the $N(\text{Fe II})/N(\text{H I})$ ratio, because of the non negligible upward correction for iron (Table 1). The upward correction for zinc is lower, and interestingly it nearly compensates the difference between [Fe/H] and [Zn/H] discussed by Prochaska & Wolfe (2000). Then, the age-metallicity relation for damped Ly α galaxies is more consistent with that for thick disk stars of our Galaxy. The opposite situation is of course realised if the neutral gas has the same metallicity as the ionized gas. In this case the observed Fe/H ratio is higher than real because in ionized gas $x(\text{Fe}^+) > x(\text{H}^0)$ while in neutral gas $x(\text{Fe}^+) = x(\text{H}^0) = 1$. As we will show below, it is, however, difficult to adjust all observed heavy element abundance ratios in the frame of the model with similar metallicities of neutral and ionized gas.

3.3. Ionization vs Dust Depletion

There is little doubt that some depletion of heavy elements by dust is present in DLAs. However, the level of depletion in DLAs is generally smaller than

that in the disk and possibly in the halo of our Galaxy. Pettini et al. (2000) adopt the model of DLA consisting only of neutral gas and propose for DLAs with low level of depletion (systems with typically $[\text{Zn}/\text{Fe}] \lesssim 0.3$) to correct abundances of refractory elements assuming constant depletion factors for all these elements. This approach obviously leaves the question open how to explain observed abundances in systems with more depletion. Besides that, the similarity of the line profiles of singly ionized ions and Al III and the large $N(\text{Al III})/N(\text{Al II})$ ratio is not addressed.

Prochaska & Wolfe (1999) have suggested that if the overabundance of Si/Fe relative to solar is indicative of dust depletion, then one might expect a correlation between [Si/Fe] and [Zn/Fe] with the most heavily depleted regions showing the largest Si/Fe and Zn/Fe ratios. Indeed, they found such correlation and concluded that this appearance is consistent with that expected for dust depletion (their Fig. 23).

Alternatively, as shown in Fig. 2, the regression between [Si/Fe] and [Zn/Fe] can be explained by ionization effects. Dashed, solid and dotted lines in Figure connect theoretical points $[x(\text{Si}^+)/x(\text{Fe}^+), x(\text{Zn}^+)/x(\text{Fe}^+)]$ in models with $Z = 0.1 Z_\odot$ calculated for various U values and for three values $T_{\text{eff}} = 33000 \text{ K}, 40000 \text{ K}$ and 45000 K of the effective temperature characterising the hardness of the ionizing radiation. Note that $[x(\text{Si}^+)/x(\text{Fe}^+)]^{-1}$ and $[x(\text{Zn}^+)/x(\text{Fe}^+)]^{-1}$ are the correction factors to convert respectively Si^+/Fe^+ to Si/Fe and Zn^+/Fe^+ to Zn/Fe and they are independent on the intrinsic abundances of Si, Fe and Zn as far as these elements do not contribute significantly to the thermal balance of the ionized gas. However, the correction factors for the considered ions can depend on the helium and the total heavy element abundances which regulate the thermal balance and the ionization structure. As mentioned above, the values of the ionization fractions x are essentially metallicity independent for heavy element mass fractions $Z \sim 0.1 - 0.01 Z_\odot$. We point out that the quantities commonly (e.g. Prochaska & Wolfe 1999) denoted as [Si/Fe] and [Zn/Fe] are actually

$$[\text{Si}/\text{Fe}] = \log[N(\text{Si II})/N(\text{Fe II})] - \log(\text{Si}/\text{Fe})_\odot \quad (3)$$

and

$$[\text{Zn}/\text{Fe}] = \log[N(\text{Zn II})/N(\text{Fe II})] - \log(\text{Zn}/\text{Fe})_\odot, \quad (4)$$

respectively. The total abundance ratios are then de-

defined as

$$[\text{Si}/\text{Fe}]_{\text{cor}} = [\text{Si}/\text{Fe}] - \log[x(\text{Si}^+)/x(\text{Fe}^+)] \quad (5)$$

and

$$[\text{Zn}/\text{Fe}]_{\text{cor}} = [\text{Zn}/\text{Fe}] - \log[x(\text{Zn}^+)/x(\text{Fe}^+)]. \quad (6)$$

We find that both the observed range of $x(\text{Al}^{+2})/x(\text{Si}^+)$ and $[\text{Zn}/\text{Fe}]$ are consistent with same ionization parameter for the ionizing radiation with $T_{\text{eff}} = 33000\text{K}$ and 40000K . Figure 2 shows that if one applies the correction for ionization effects for the radiation effective temperature of 40000K , assuming that after correction $[\text{Zn}/\text{Fe}]_{\text{cor}} = 0$, the resulting $[\text{Si}/\text{Fe}]_{\text{cor}}$ value remains on average above zero with a small spread of points (see also Fig. 4), and no additional correction for dust depletion is required. However, models with harder radiation with $T_{\text{eff}} = 45000\text{K}$ do not reproduce the observed trend. If our approach is correct then we obtain important constraint on the hardness of the ionizing stellar radiation in DLAs from Figure 2. Note that with the hard intergalactic background radiation field considered by Howk & Sembach (1999) the observed $[\text{Zn}/\text{Fe}]$ vs $[\text{Si}/\text{Fe}]$ relation cannot be reproduced because of their adopted boundary conditions. In this case (see their Fig. 1) the correction for ionization of $[\text{Zn}/\text{Fe}]$ is positive, while that of $[\text{Si}/\text{Fe}]$ is negative. Even if an ionization bounded model with the hard intergalactic background radiation field is considered, the correction for ionization of $[\text{Zn}/\text{Fe}]$, though smaller, remains positive. In our case both corrections are negative.

In summary, it is possible to reproduce the observed $N(\text{Al III})/N(\text{Si II})$ ratios and the trend seen in $[\text{Si}/\text{Fe}]$ vs $[\text{Zn}/\text{Fe}]$ diagram assuming ionization by a moderately hard stellar ionizing radiation field. In principle, no correction for dust depletion needs to be invoked, although it might be present in small amounts and can easily be taken into account in the ionization model without significant changing the main features of the $[\text{Si}/\text{Fe}]$ vs $[\text{Zn}/\text{Fe}]$ distribution.

Additional support of the ionization model comes from Fig. 3 where we show the dependence of $[\text{Al III}/\text{Fe II}]$ vs $[\text{Zn II}/\text{Fe II}]$. Models with $T_{\text{eff}} = 33000\text{K}$ (dashed line) and 40000K (solid line) fit quite well the observed points from Prochaska & Wolfe (1999) and Lu et al. (1996a) at the values of ionization parameter U close to that obtained from Fig. 2.

3.4. Abundance ratios in ionization bounded DLAs

The above conclusion is broadly consistent with expectations for other heavy element abundance ratios. To illustrate this we apply a “typical” ionization correction factor to the observational data. To do so we adopt the characteristic correction factors of the model with gas ionized by the radiation with $T_{\text{eff}} = 40000\text{K}$. We consider the metallicity $Z = 0.1 Z_{\odot}$ as representative for the sample of DLA systems and adopt $\log U = -3.25$. Then, our calculations yield the following mean ionization correction factors $\Delta \log[X/\text{H}]$ defined by $\log[X/\text{H}]_{\text{corrected}} = \log[X/\text{H}]_{\text{observed}} + \Delta \log[X/\text{H}]$: $\Delta \log[\text{Al}/\text{Fe}] = -0.63$, $\Delta \log[\text{Si}/\text{Fe}] = -0.31$, $\Delta \log[\text{S}/\text{Fe}] = -0.32$, $\Delta \log[\text{Ti}/\text{Fe}] = -0.12$, $\Delta \log[\text{Cr}/\text{Fe}] = +0.16$, $\Delta \log[\text{Mn}/\text{Fe}] = -0.01$, $\Delta \log[\text{Ni}/\text{Fe}] = -0.38$, $\Delta \log[\text{Zn}/\text{Fe}] = -0.40$. Note the small corrections for $[\text{Ti}/\text{Fe}]$ and $[\text{Mn}/\text{Fe}]$ which remain almost unchanged while the downward correction of $[\text{Zn}/\text{Fe}]$ is high. Interestingly, it is the same as the difference between mean $[\text{Fe}/\text{H}]$ and $[\text{Zn}/\text{H}]$ values for DLAs at $z \approx 2$ from Prochaska & Wolfe (2000). The case of nitrogen is discussed separately below.

The above “typical” correction factors have been applied to the sample of damped Ly α galaxies from Lu et al. (1996a), Prochaska & Wolfe (1999) and Pettini et al. (2000). Only galaxies with definitely derived column densities are included and we do not consider objects with lower or upper limits. The original (open symbols) and corrected (filled symbols) abundance ratios are shown in Fig. 4. As pointed out earlier, an upward correction of $[\text{Fe}/\text{H}]$ must also be applied because of the large column density of neutral hydrogen. However, this correction is uncertain and does not change the relative heavy element abundances. Therefore, we simply use $[\text{Fe}/\text{H}]$ values derived by Lu et al. (1996a), Prochaska & Wolfe (1999) and Pettini et al. (2000) keeping in mind that correction might be up to of the order of +1 dex. For 4 DLAs of the sample the $[\text{Fe}/\text{H}]$ are not available. We adopt $[\text{Fe}/\text{H}] = [\text{Cr}/\text{H}]$ for those systems. For $[\text{Ni}/\text{Fe}]$ we have applied an additional upward correction which comes from the new measurements of oscillator strengths for Ni II from UV absorption lines (Fedchak & Lawler 1999); older f -values were used by Prochaska & Wolfe (1999) and Lu et al. (1996a). Although the correction is different for different Ni II transitions, its mean value is ~ 0.3 dex, which we adopt for the sake of simplicity. We now discuss the behaviour of the element ratios of Si, Zn, S, Mn, Cr, Ni, Ti, and Al with respect to

Fe.

Silicon, Zinc: The case of Si and Zn has already been treated before (Sect. 3.3). In short, it can be seen from Fig. 4 that the corrected $[\text{Zn}/\text{Fe}]$ values scatter around zero, while $[\text{Si}/\text{Fe}]$ remains positive suggesting the production of this element in Type II supernovae.

Sulphur: $[\text{S}/\text{Fe}]$ shows the same SNII like pattern as $[\text{Si}/\text{Fe}]$. We note that if the gas in DLA galaxies is ionized by softer stellar radiation with $T_{\text{eff}} = 33000$ K, the downward correction of S/Fe abundance ratio is 0.17 dex larger and in this case $[\text{S}/\text{Fe}] < 0$, in contradiction with the production of S in Type II supernovae. This difference in S correction factors also favours harder ionization radiation for the low-metallicity DLAs as compared to that in the Milky Way. A new analysis of the S/Zn abundance ratio in a sample of DLAs was recently presented by Centurión et al. (2000). They find $[\text{S}/\text{Zn}] < 0$ in DLAs with $[\text{Zn}/\text{H}] \gtrsim -1.0$. Both S and Zn are not depleted into the dust grains and the correction for dust depletion does not change S/Zn ratio. Centurión et al. (2000) thus conclude that such unusual abundance ratios suggest that the DLA galaxies are objects with low star formation rates such as low surface brightness galaxies or dwarf galaxies. Based on our model, the correction for the ionization results in the increase of both $[\text{S}/\text{Zn}]$ (Table 1) and $[\text{Zn}/\text{H}]$ and in better agreement with $[\text{S}/\text{Fe}]$ for halo stars. If instead the model with the hard background intergalactic radiation is adopted, the correction of $[\text{S}/\text{Zn}]$ is negative and it increases the difference between $[\text{S}/\text{Zn}]$ in DLAs and $[\text{S}/\text{Fe}]$ in halo stars.

Manganese, Chromium: $[\text{Mn}/\text{Fe}]$ remains nearly unchanged because of small correction factor for this ratio. The Cr/Fe ratio is overabundant by ~ 0.2 dex with respect to the solar value, which seems to be in contradiction with the stellar data. This may constitute a difficulty for our model. Uncertainties in oscillator strengths for Cr II transitions are better than 10% (Bergeson & Lawler (1993)). However uncertainties in the ionization and recombination cross-sections should be examined. Adopting a higher effective temperature decreases the overabundance of Cr relative to Fe, as can be seen from Table 1. The Mn/Fe ratio remains underabundant supporting the origin of this odd-element in Type II supernovae.

Nickel: Note that $[\text{Ni}/\text{Fe}]$ calculated with the new oscillator strengths before the ionization correction (open circles) are already above zero. This poses

a problem in the explanation of $[\text{Ni}/\text{Fe}]$ when dust depletion is taken into account, since this correction shifts the points upward. Although a large negative correction of -0.38 is predicted for $[\text{Ni}/\text{Fe}]$ in the ionization model, it is almostly compensated by the upward shift of points introduced by the new oscillator strengths by Fedchak & Lawler (1999). The points in $[\text{Ni}/\text{Fe}]$ vs $[\text{Fe}/\text{H}]$ diagram scatter around the mean $[\text{Ni}/\text{Fe}]$ value of -0.2 .

Titanium: Prochaska & Wolfe (1999) pointed out problems in explaining the Ti/Fe abundance ratio in the “dust depletion” model, since Ti is expected to be more heavily incorporated into dust grains. Hence, the correction for depletion shifts observed $[\text{Ti}/\text{Fe}]$ to larger values. In our model, the correction of $[\text{Ti}/\text{Fe}]$ for ionization effects is negative and small. Therefore, its application to Prochaska & Wolfe (1999) data leaves Ti moderately overabundant relative to iron (filled squares in Fig. 4), in agreement with that observed in galactic halo stars.

Aluminium: Our model predicts the largest downward correction factor of -0.63 dex for Al/Fe abundance ratio. In the Prochaska & Wolfe (1999) sample the $[\text{Al}/\text{Fe}]$ scatter around zero value. This is likely at variance with what is observed in lowest-metallicity halo stars where $[\text{Al}/\text{Fe}]$ scatters below zero with mean value of ~ -0.4 (Ryan et al. 1996; Timmes et al. 1995; Samland 1998). Our correction eliminates this difference and suggests that the odd-element Al seen in damped Ly α galaxies is likely also produced by Type II supernovae. If instead the hard intergalactic ionization radiation is applied, the correction of $[\text{Al}/\text{Fe}]$ is $\sim +0.1$ and shifts points upward in the direction opposite to the nucleosynthetic predictions.

Overall, we find that in the framework of our simplified model of photoionized gas and despite the uncertainties in the atomic data, the abundances in DLA systems reproduce quite well observed halo star abundance patterns and lead to a consistent picture. Several problems pertaining to neutral DLA models are thus eliminated. In the new model, there is no need to take depletion of heavy elements into dust grains into account, although small depletion of heavy elements might be present.

In the framework of the proposed model the abundance ratios of neutral and singly ionized species N I / O I, Si II / S II, Mn II / Fe II (Table 1) depend only weakly on ionization effects and can be used as a good measure of the total abundance ratios.

3.5. On the origin of nitrogen

We now turn to a discussion of the nitrogen abundance, which is of particular interest since it is one of the elements observable both in metal-poor HII regions and DLAs, and because its primary and/or secondary origin remains debated (see e.g. Henry, Edmunds & Köppen 2000).

The heavy element abundance patterns seen in DLA galaxies show several similarities with those found in local blue compact dwarf galaxies. Izotov & Thuan (1999), based on the large sample of low-metallicity BCDs, have demonstrated that all elements of α process are overabundant relative to iron and hence they are produced in Type II supernovae.

In this respect the N/O ratios seem, at first glance, to constitute the major difference. The N/O ratios in damped Ly α systems appear to be significantly lower than those measured in low-metallicity BCDs (cf. Fig. 5). For the most metal deficient of these objects with $[O/H] \lesssim -1.3$ Thuan, Izotov & Lipovetsky (1995) and Izotov & Thuan (1999) have derived a mean value of $\log N/O = -1.60$ with a very small dispersion. They argue that this value constitutes a lower limit to $\log N/O$ in BCDs, which is set by primary N production in massive stars. Pettini, Lipman & Hunstead (1995) have found an upper limit $\log N/O \lesssim -1.9$ in one damped Ly α system, 0.3 dex below the value of Izotov & Thuan. However, within the errors the $\log N/O$ value derived by Pettini et al. (1995) is still consistent with the mean value for BCDs. Furthermore, Lu, Sargent & Barlow (1998) have compiled N/Si abundance ratios in 15 damped Ly α galaxies, and have set upper limits for $\log N/O$ ranging from -1.2 to -2.1 . Whereas all these measurements constitute upper limits, an actual value of $[N/Si] = -1.70$ has been derived in one system, 1946+7658, by Lu et al. (1998). From these DLA measurements of N/O and N/Si, Pettini et al. (1995) conclude that both primary and secondary nitrogen production are important over the whole range of metallicity measured in damped Ly α systems, while Lu et al. (1998) favor the time-delayed primary nitrogen production by intermediate-mass stars.

Can these different scenarios be reconciled? How well are these differences established, especially in view of the possible ionization corrections discussed above for other elements detected in DLA systems? Indeed if our model holds, ionization effects are also important for the N/Si abundance ratio. The

inspection of Table 1 and Figure 1 shows that correction factors for the observed $N(N^0)/N(Si^+)$ ratio increase with increasing U . For the typical value $\log U = -3.25$ adopted for the above analysis of other heavy element abundance ratios (cf. Fig. 4) we find $\Delta \log[x(N^0)/x(Si^+)] = 0.72$.³

The observations of N/O in BCDs (Izotov & Thuan 1999, filled circles) and the DLA data from Lu et al. (1998) and Outram et al. (1999) (open circles) assuming neutral systems are plotted in Figure 5. Overplotted for illustration is the contribution of primary and secondary nitrogen production as well as the combined production by both mechanisms. The “typical” ionization correction for N/Si and Si/H⁴ is shown by the arrow in the lower left corner of Figure 5. Taking into account such a correction, the vast majority of measurements for DLAs are found at or above the N/O value from the BCDs. This suggests that a significant part of the difference in $[N/Si]$ can be explained by ionization effects. The typical correction brings even the lowest value of $[N/Si] \sim -1.7$, measured in the $z_{\text{damp}} = 2.8448$ damped Ly α system toward Q1946 + 7658, to $[N/Si] \sim -0.98$ after correction for ionization, fairly close to the $[N/O]$ values for the BCDs.

The open square in Fig. 5 shows the N/O abundance ratio derived recently by Molaro et al. (2000) in a DLA with $z_{\text{abs}} = 3.3901$ from the unsaturated O I and N I absorption lines. Potentially, the N/O abundance ratio derived directly from N I and O I (instead of using Si as a proxy) is the least model-dependent. Also it has the advantage of being very little dependent on the correction for ionization (see Table 1). Most interestingly, the N/O value of Molaro et al. (2000) is in very good agreement with N/O derived in the low-metallicity BCDs.

In any case, if the typical ionization corrections derived from our model apply, we have to conclude that the bulk of the present data does not show a significant difference in N/O abundance ratios between low-metallicity BCDs and DLA systems implying similar origin of these two elements. We shall now briefly summarise recent progress in stellar models regarding the nucleosynthetic origin of nitrogen.

³In the models of Howk & Sembach (1999) the correction $\Delta \log[x(N^0)/x(Si^+)]$ is significantly larger (1.48 dex) because of the assumption of density-bounded H II region in their case.

⁴Only the correction for Si/H in ionized region is taken into account. Larger upward corrections for Si/H should be applied if neutral hydrogen region is considered.

Interestingly both intermediate-mass and massive stars are found to be potential producers of primary ^{14}N in the most recent stellar models. Intermediate mass stars ($M_{\text{initial}} \gtrsim 3.5 M_{\odot}$) produce primary nitrogen when the CN cycle operates in their convective envelope during the AGB phase (e.g. Renzini & Voli 1981). This production results from the combined effect of the 3rd dredge-up and envelope burning, and thus varies both with stellar mass and metallicity (e.g. Forestini & Charbonnel (1997) and references therein). It is also highly dependent on the parameters which intervene in the description of AGB stars. Among them, the mixing length and the dredge-up parameters which are empirically calibrated to reproduce peculiar observed properties of different AGB populations (in particular the observed luminosity function of carbon stars in the LMC and SMC), and which influence the efficiency of the burning inside the envelope. In addition, the mass loss prescription which remains uncertain (e.g. Vassiliadis & Wood 1993) has a crucial impact on the theoretical nucleosynthesis by controlling the number of thermal pulses undergone by the AGB star and the duration of the envelope burning. The most recent models find a ^{14}N production similar to that of Renzini & Voli (1981, $\alpha = 1.5$ case with the largest N production) at $[\text{O}/\text{H}] \sim -0.7$ but which decreases with increasing metallicity (see Marigo 1998; Marigo et al. 1998; Lattanzio, Forestini & Charbonnel 1999). Intermediate mass stars are thus potential primary ^{14}N producers. However, no calculations are yet available in the metallicity range of interest for our study. The behaviour at $[\text{O}/\text{H}] < -0.7$ remains to be investigated.

Regarding massive stars it is well known that standard stellar evolution models do not produce primary nitrogen (e.g. Woosley & Weaver 1995). However, considerable advances have been made recently to include rotation and its effects on the transport of elements and angular momentum in the description of stellar interiors and evolution (see review of Maeder & Meynet 2000). The corresponding new models for massive stars, which solve a number of difficulties encountered by “standard” models (cf. Maeder 1995), also produce primary nitrogen (Maeder 1999; Langer et al. 1999). In particular the models of Maeder (1999) reproduce well the N excess in SMC supergiants found by Venn (1999), and suggest that these stars could be responsible for primary N production at early epochs. Increasing rotational velocities found at low O/H (Maeder, Grebel & Mermilliod 1999) could

favor the primary N production in metal-poor environments. Quantitative yields from these new stellar models have still to be awaited.

Last, but not least, such new yields from intermediate and massive stars will be included in chemical evolution models to fully exploit all the observational constraints regarding N and other elements. This should hopefully solve the question on the origin of primary N. Independently of the outcome, the conclusion from our work is that in the light of possible ionization corrections for DLAs one cannot presently exclude the same primary origin of N in both DLAs and nearby metal-poor galaxies.

4. DISCUSSION AND SUMMARY

The above analysis shows the importance of consideration of the ionization effects in the DLAs element abundance studies which was pointed out earlier by Prochaska & Wolfe (1999), Howk & Sembach (1999) and Izotov & Thuan (1999). However, at variance with many previous studies assuming that the heavy element absorption lines in DLA galaxies are formed in the neutral gas, we consider the following simplified “multi-component” picture for DLA systems: *Region 1*) A plane-parallel ionization bounded region illuminated by an internal radiation field complemented by *Region 2*), a neutral region with a lower metal content.

Interestingly it appears that the structure of at least some DLA systems might be similar to that observed in nearby low-metallicity blue compact dwarf galaxies. For example, the BCD galaxy SBS 0335–052 showing supergiant H II regions over a region of ~ 7 kpc with ongoing star formation embedded in much larger clouds of neutral gas with a column density $N(\text{H I})$ as high as $7 \times 10^{21} \text{ cm}^{-2}$, can be considered as a local damped Ly α system (e.g., Thuan & Izotov 1997).

Another interesting parallel is the most metal-poor BCD galaxy I Zw 18, which shows a high hydrogen column density $N(\text{H I}) \approx 3.5 \times 10^{21} \text{ cm}^{-2}$ (Kunth et al. 1994) thus also qualifying as a local DLA system, and for which recent *FUSE* spectroscopic observations were obtained by Vidal-Madjar et al. (2000). In contrast with high-redshift DLAs the structure of I Zw 18 is known better. It consists of two central regions of active star formation ionizing the ambient gas. Radio observations and the presence of strong Ly α absorption line indicate that the H II region is

embedded in the outer H I cloud. Measurements of the column densities of N I, Si II, Ar I and Fe II derived from the *FUSE* spectrum of I Zw 18 were kindly made available to us by Alfred Vidal-Madjar (2000, private communication). It is striking that the column density ratios given in Table 2 (column 2) are very different from those observed in the H II regions (NW and SE components) of I Zw 18 and other low-metallicity BCDs also given in the Table 2. We suspect that such large differences are due to ionization effects. To analyse the influence of the ionization on the observed column densities we consider a spherically-symmetric ionization-bounded H II region model with the parameters derived from the observations (see e.g. Hunter & Thronson 1995; De Mello et al. 1998). In particular, the heavy element mass fraction in H II region is adopted to be $1/50 Z_{\odot}$, while for the neutral gas we assume zero metallicity.

The results of the calculations are shown in Table 2, where the observed ratio from *FUSE* (col. 2) and the ionization corrected column density ratio (col. 3) are given. Note the good agreement with the abundance ratios derived from the *HST* and ground-based observations of I Zw 18 and other BCDs, while solar ratios do not match corrected ratios. To obtain the total hydrogen column density a large amount of gas must now be added to that of the ionized gas (cf. Table 2). However, since the heavy element ratios are already close to the observed values from the H II regions in BCDs, there is little room for additional metals in the neutral phase. Hence, this analysis provides some support in favor of the basic assumption of our model that neutral gas in DLAs systems might be more metal-poor as compared to the ionized gas.

From our simplified model (see Sect. 2) the following main results are obtained (Sect. 3):

1. Using the observed $N(\text{Al III})/N(\text{Si II})$ column density ratio to constrain the ionization parameter U , one obtains almost complete ionization of hydrogen in regions with a column density $N(\text{H}^0 + \text{H}^+) \sim 10^{20} \text{ cm}^{-2}$ (region 1), several times smaller than the observed HI column in DLA systems. In the ionized region Fe is mainly in the Fe^{+2} form. Both effects imply that the true Fe/H abundance in the ionized gas must be larger (by up to one order of magnitude) than that derived from the $N(\text{Fe II})/N(\text{H I})$ ratio. Compared to $[\text{Fe}/\text{H}]$ derived from a neutral DLA model, such ionized systems have an age-metallicity relation in better agreement with that of the thick disk of the Milky Way. However, in general, due to the assump-

tion of a significant metal-deficiency in the neutral region (2), abundance ratios with respect to hydrogen are a priori not meaningful when the total absorbing column is taken into account.

2. Accounting for ionization effects improves the agreement between DLAs and Milky Way stellar thick disk measurements. Although not excluded, no significant depletion of elements by dust grains is required. The majority of heavy element abundance ratios are brought into agreement with those expected from the production by Type II supernovae. The apparent difference between $[\text{N}/\text{O}]$ derived in local blue compact dwarf galaxies and $[\text{N}/\text{Si}]$ derived in DLA systems can be fairly well explained by ionization effects in the latter. Thus one cannot currently exclude the same primary N origin in both DLAs and metal-poor galaxies.

The above findings lead to a more consistent picture for the heavy element pattern in DLAs, and render our simple model attractive.

The main sources of uncertainties potentially affecting our results are: poor atomic data (oscillator strengths, recombination coefficients etc. for the photoionization models, affecting e.g. Zn, Cr, and Ni), the unknown structure and geometry of the absorbing systems, the spatial distribution of ionizing sources and their radiation field, and uncertainties related to the measurement of column densities. Future investigations should hopefully be able to improve on these issues and to assess the validity of our picture. For example, quantitative studies of the line profile structure of different ions, and detailed ionization properties of individual systems and large samples, should be extremely useful. It is the hope that the proposed simplified model reflects the main trends due to ionization effects in DLAs. If correct, our picture of DLA systems partly ionized by internal radiation offers a clear simplification in the understanding of heavy element abundance ratios in DLAs and their comparison with the local Universe.

Y.I.I. thanks the staff of the Observatoire Midi-Pyrénées for their kind hospitality, and acknowledges an invitation by the Université Paul Sabatier in Toulouse. Alfred Vidal-Madjar kindly provided us with results of *FUSE* observations. We thank Richard F. Green and an anonymous referee for useful comments on this paper. This international collaboration was possible thanks to the partial financial support of INTAS grant No. 97-0033 for which Y.I.I.

and D.S. are grateful. Y.I.I. acknowledges the partial financial support of the Joint Research Project between Eastern Europe and Switzerland (SCOPE) No. 7UKPJ62178.

REFERENCES

- Anders, S., & Grevesse, N. 1989, *Geochim. Cosmochim. Acta*, 53, 197
- Bergeson, S. D., & Lawler, J. E. 1993, *ApJ*, 408, 382
- Centurión, M., Bonifacio, P., Molaro, P., & Vladilo, G. 2000, *ApJ*, 536, 540
- De Mello, D. F., Schaerer, D., Heldmann, J., & Leitherer, C. 1998, *ApJ*, 507, 199
- Fedchak, J. A., & Lawler, J. E. 1999, *ApJ*, 523, 734
- Ferland, G. J. 1996, HAZY, A Brief Introduction to CLOUDY 90 (University of Kentucky, Department of Physics and Astronomy, Internal Report)
- Ferland, G. J., Korista, K. T., Verner, D. A., Ferguson, J. W., Kingdon, J. B., & Verner, E. M. 1998, *PASP*, 110, 761
- Forestini, M., & Charbonnel, C. 1997, *A&AS*, 123, 241
- Henry, R. B. C., Edmunds, M. G., & Köppen, J. 2000, *ApJ*, 541, 660
- Howk, J. C., & Sembach, K. R. 1999, *ApJ*, 523, L141
- Howk, J. C., Savage, B. D., & Fabian, D. 1999, *ApJ*, 525, 253
- Hunter, D. A., & Thronson, H. A., Jr. 1995, *ApJ*, 452, 238
- Izotov, Y. I., Chaffee, F. H., Foltz, C. B., Green, R. F., Guseva, N. G., & Thuan, T. X. 1999, *ApJ*, 525, 757
- Izotov, Y. I., & Thuan, T. X. 1998, *ApJ*, 500, 188
- . 1999, *ApJ*, 511, 639
- Jenkins, E. B., Oegerle, W. R., Gry, C., Vallerga, J., Sembach, K. R., Shelton, R. L., Ferlet, R., Vidal-Madjar, A., York, D. G., Linsky, J. L., Roth, K. C., Dupree, A. K., & Edelstein, J. 2000, *ApJ*, 538, L81
- Kunth, D., Lequeux, J., Sargent, W. L. W., & Viallefond, F. 1994, *A&A*, 282, 709
- Kurucz, R. L. 1991, in *Proc. Workshop on Precision Photometry: Astrophysics of the Galaxy*, ed. A. C. Davis Philip, A. R. Upgren, & K. A. James (Schenectady: Davis), 27
- Langer, N., Heger, A., Woosley, S. E., & Herwig, F. 1999, in *Nuclei in the Cosmos*, ed. N. Prantzos, in press
- Lanzetta, K. M., Wolfe, A. M., & Turnshek, D. A. 1995, *ApJS*, 440, 435
- Lattanzio, J., Forestini, M., & Charbonnel, C., 1999, in *International Workshop on “The changes in abundances in AGB stars”*, Monteporzio, in press (astro-ph/9912298)
- Lauroesch, J. T., Truran, J. W., Welty, D. E., & York, D. G. 1996, *PASP*, 108, 641
- Le Brun, V., Bergeron, G., Boissé, P., & Deharveng, J. M. 1997, *A&A*, 321, 733
- Lindner, U., Fritze - von Alvensleben, U., & Fricke, K. J. 1999, *A&A*, 341, 709
- Lu, L., Sargent, W. L. W., & Barlow, T. A. 1998, *AJ*, 115, 55
- Lu, L., Sargent, W. L. W., Barlow, T. A., Churchill, C. W., & Vogt, S. S. 1996a, *ApJS*, 107, 475
- Lu, L., Sargent, W. L. W., Womble, D. S., & Barlow, T. A. 1996b, *ApJ*, 457, L1
- Maeder, A. 1995, in *Astrophysical Applications of Stellar Pulsation*, ed. R.S. Stobie, P.A. Whitelock, ASP Conf. Series, 83, 1
- Maeder, A. 1999, in *Wolf-Rayet Phenomena in Massive Stars and Starburst Galaxies*, ed. K. A. van der Hucht, G. Koenigsberger, & P. R. J. Eenens (Sheridan Books: Michigan), 177
- Maeder, A., & Meynet, G. 2000, *ARA&A*, in press
- Maeder, A., Grebel, E. K., & Mermilliod, J.-C. 1999, *A&A*, 346, 459
- Marigo, P. 1998, PhD thesis, Universita de Padova
- Marigo, P., Bressan, A., & Chiosi, C. 1998, *A&A*, 331, 564
- Molaro, P., Bonifacio, P., Centurión, M., D’Odorico, S., Vladilo, G., Santin, P., & Di Marcantonio, P. 2000, *ApJ*, 541, 54
- Outram, P. J., Chaffee, F. H., & Carswell, R. F. 1999, *MNRAS*, 310, 289
- Pettini, M., Ellison, S. L., Steidel, C. C., & Bowen, D. V. 1999, *ApJ*, 510, 576
- Pettini, M., Ellison, S. L., Steidel, C. C., Shapley, A. E., & Bowen, D. V. 2000, *ApJ*, 532, 65
- Pettini, M., King, D. L., Smith, L. J., & Hunstead, R. W. 1997, *ApJ*, 478, 536

- Pettini, M., Lipman, K., & Hunstead, R. W. 1995, *ApJ*, 451, 100
- Pettini, M., Smith, L. J., Hunstead, R. W., & King, D. L. 1994, *ApJ*, 426, 79
- Prantzos, N., & Boissier, S. 2000, *MNRAS*, 315, 82
- Prochaska, J., & Wolfe, A. M. 1996, *ApJ*, 470, 403
- . 1999, *ApJS*, 121, 369
- . 2000, *ApJ*, 533, L5
- Renzini, A., & Voli, M. 1981, *A&A*, 94, 175
- Ryan, S. G., Norris, J. E., & Beers, T. C. 1996, *ApJ*, 471, 254
- Samland, M. 1998, *ApJ*, 496, 155
- Sembach, K. R., Howk, J. C., Ryans, R. S. I., & Keenan, F. P. 2000, *ApJ*, 528, 310
- Stasińska, G., & Leitherer, C. 1996, *ApJS* 107, 661
- Thuan, T. X., & Izotov, Y. I. 1997, *ApJ*, 489, 623
- Thuan, T. X., Izotov, Y. I., & Lipovetsky, V. A. 1995, *ApJ*, 445, 108
- Timmes, F. X., Woosley, S. E., & Weaver, T. A. 1995, *ApJS*, 98, 617
- Vassiliadis, E., & Wood, P. R. 1993, *ApJ*, 413, 641
- Venn, K. A. 1999, *ApJ*, 518, 405
- Vidal-Madjar, A. 2000, private communication
- Vidal-Madjar, A., Kunth, D., Lecavelier des Etangs, A., Lequeux, J., André, M., BenJaffel, L., Fernet, R., Hébrard, G., Howk, J. C., Kruk, J. W., Lemoine, M., Moos, H. W., Roth, K. C., Sonneborn, G., & York, D. G. 2000, *ApJ*, 538, L77
- Viegas, S. M. 1995, *MNRAS*, 276, 268
- Vladilo, G. 1998, *ApJ*, 493, 583
- Wolfe, A. M. 1990, in *The Interstellar Medium in Galaxies*, ed. H. A. Thronson & J. M. Shull (Dordrecht: Kluwer), 387
- Wolfe, A. M., Lanzetta, K. M., Foltz, C. B., & Chaffee, F. H. 1995, *ApJ*, 454, 698
- Wolfe, A. M., & Prochaska, J. X. 2000, *ApJ*, in press (preprint astro-ph/0009081)
- Woosley, S. E., & Weaver, T. A. 1995, *ApJS*, 101, 181

TABLE 1
 IONIC ABUNDANCE FRACTIONS FOR $Z=10^{-1}Z_{\odot}$

Property	IP ^a	$T_{\text{eff}}=33000\text{K}$					$T_{\text{eff}}=40000\text{K}$				
		$\log U=-5.0$	-4.0	-3.5	-3.0	-2.0	$\log U=-5.0$	-4.0	-3.5	-3.0	-2.0
$N(\text{H}^0+\text{H}^+)$		5.24×10^{18}	1.78×10^{19}	4.49×10^{19}	1.31×10^{20}	1.30×10^{21}	6.38×10^{18}	1.95×10^{19}	4.56×10^{19}	1.29×10^{20}	1.27×10^{21}
$\log x(\text{H}^0)$	1.00	-0.186	-0.551	-0.888	-1.297	-2.195	-0.154	-0.455	-0.785	-1.224	-2.172
$\log x(\text{He}^0)$	1.81	-0.008	-0.029	-0.040	-0.047	-0.044	-0.097	-0.321	-0.581	-0.897	-1.193
$\log x(\text{C}^0)$	0.83	-1.686	-2.420	-2.858	-3.346	-4.440	-1.335	-2.086	-2.579	-3.202	-4.660
$\log x(\text{C}^+)$	0.83,1.79	-0.009	-0.004	-0.006	-0.016	-0.118	-0.024	-0.037	-0.111	-0.279	-0.795
$\log x(\text{C}^{+3})$	3.52,4.74	-5.638	-4.206
$\log x(\text{N}^0)$	1.07	-0.205	-0.595	-0.947	-1.376	-2.305	-0.184	-0.506	-0.852	-1.317	-2.333
$\log x(\text{N}^+)$	1.07,2.18	-0.424	-0.127	-0.052	-0.020	-0.015	-0.461	-0.168	-0.110	-0.211	-0.730
$\log x(\text{O}^0)$	1.00	-0.176	-0.534	-0.870	-1.278	-2.183	-0.145	-0.441	-0.770	-1.210	-2.182
$\log x(\text{Mg}^0)$	0.56	-2.290	-2.548	-2.974	-3.577	-5.013	-2.242	-2.449	-2.711	-3.218	-4.580
$\log x(\text{Mg}^+)$	0.56,1.11	-0.011	-0.069	-0.192	-0.431	-1.153	-0.011	-0.068	-0.200	-0.451	-1.153
$\log x(\text{Al}^+)$	0.44,1.38	-0.001	-0.005	-0.013	-0.036	-0.229	-0.002	-0.007	-0.019	-0.052	-0.396
$\log x(\text{Al}^{+2})$	1.38,2.09	-2.740	-1.991	-1.540	-1.104	-0.389	-2.533	-1.838	-1.397	-0.991	-0.521
$\log x(\text{Si}^+)$	0.60,1.20	-0.004	-0.071	-0.225	-0.491	-1.133	-0.004	-0.068	-0.226	-0.501	-1.113
$\log x(\text{Si}^{+3})$	2.46,3.32	-6.061	-5.351	-4.147	...	-4.570	-3.423	-2.612	-1.489
$\log x(\text{P}^+)$	0.77,1.45	-0.008	-0.025	-0.080	-0.221	-0.830	-0.017	-0.034	-0.109	-0.318	-0.935
$\log x(\text{S}^+)$	0.76,1.72	-0.008	-0.039	-0.114	-0.293	-0.995	-0.017	-0.078	-0.220	-0.485	-1.243
$\log x(\text{S}^{+2})$	1.72,2.56	-1.894	-1.075	-0.637	-0.309	-0.046	-1.602	-0.789	-0.402	-0.173	-0.034
$\log x(\text{Ar}^0)$	1.16	-0.461	-0.900	-1.270	-1.709	-2.657	-0.470	-0.799	-1.160	-1.647	-2.698
$\log x(\text{Ti}^+)$	0.50,1.00	-0.022	-0.157	-0.372	-0.698	-1.516	-0.023	-0.153	-0.380	-0.738	-1.619
$\log x(\text{Cr}^+)$	0.50,1.21	-0.057	-0.358	-0.675	-1.054	-1.874	-0.052	-0.315	-0.627	-1.035	-1.948
$\log x(\text{Mn}^+)$	0.55,1.15	-0.058	-0.263	-0.504	-0.793	-1.499	-0.057	-0.242	-0.494	-0.832	-1.652
$\log x(\text{Fe}^+)$	0.58,1.19	-0.032	-0.219	-0.495	-0.869	-1.726	-0.026	-0.198	-0.475	-0.873	-1.804
$\log x(\text{Fe}^{+2})$	1.19,2.25	-1.160	-0.402	-0.167	-0.063	-0.016	-1.263	-0.439	-0.186	-0.127	-0.602
$\log x(\text{Co}^+)$	0.58,1.26	-0.006	-0.023	-0.143	-0.477	-1.394	-0.006	-0.025	-0.159	-0.505	-1.383
$\log x(\text{Ni}^+)$	0.56,1.34	-0.006	-0.016	-0.113	-0.427	-1.350	-0.006	-0.019	-0.138	-0.474	-1.346
$\log x(\text{Cu}^+)$	0.57,1.49	-0.015	-0.149	-0.386	-0.744	-1.621	-0.020	-0.177	-0.437	-0.813	-1.707
$\log x(\text{Zn}^+)$	0.69,1.32	-0.006	-0.005	-0.012	-0.034	-0.234	-0.017	-0.063	-0.170	-0.375	-0.888

^aIonization potential of the X^{i-1} ion (first value) and X^i ion (second value) expressed in Ryd.

TABLE 2
 ABUNDANCE RATIOS IN I Zw 18 FROM *FUSE*, *HST* AND GROUND-BASED OBSERVATIONS

	<i>FUSE</i> ^a	Model	I Zw 18 (NW) ^b	I Zw 18 (SE) ^b	BCDs ^c	Sun ^d
$N(\text{H}), \text{cm}^{-2}$	$2.1 \times 10^{21\text{e}}$	$7.7 \times 10^{20\text{f}}$
D, Mpc^{g}	...	10
$\log Q, \text{s}^{-1\text{h}}$...	51.6
$\log R_{\text{in}}, \text{cm}^{\text{i}}$...	20.08
$T_{\text{eff}}, \text{K}^{\text{j}}$...	50000
$N, \text{cm}^{-3\text{k}}$...	100
f^{l}	...	0.1
$\log \text{N}/\text{Si}^{\text{m}}$	-0.77	-0.14	...	-0.09 ± 0.23	-0.10 ± 0.06	+0.32
$\log \text{Ar}/\text{Si}^{\text{m}}$	-1.32	-0.57	-0.61 ± 0.22	-0.74 ± 0.22	-0.72 ± 0.09	-0.95
$\log \text{Fe}/\text{Si}^{\text{m}}$	-0.77	-0.42	...	-0.41 ± 0.24	-0.45 ± 0.12	-0.04

^aVidal-Madjar et al. (2000), Vidal-Madjar (2000, private communication).

^bSi abundance is from Izotov & Thuan (1999), abundances of other elements are from Izotov et al. (1999).

^cMean abundance ratios for the BCDs with oxygen abundance $12 + \log \text{O}/\text{H} \leq 7.60$ (Izotov & Thuan 1999).

^dAnders & Grevesse (1989).

^eNeutral hydrogen column number density.

^fIonized hydrogen column number density.

^gThe distance to I Zw 18.

^hTotal number of the ionizing photons.

ⁱInner radius of the ionized shell.

^jEffective temperature of the ionizing radiation.

^kNumber density in H II region.

^lVolume filling factor.

^mSecond column: column density ratios $N(\text{NI})/N(\text{SiII})$, $N(\text{ArI})/N(\text{SiII})$, $N(\text{FeII})/N(\text{SiII})$ (dex) from the *FUSE* observations. Other columns: total abundance ratios (dex).

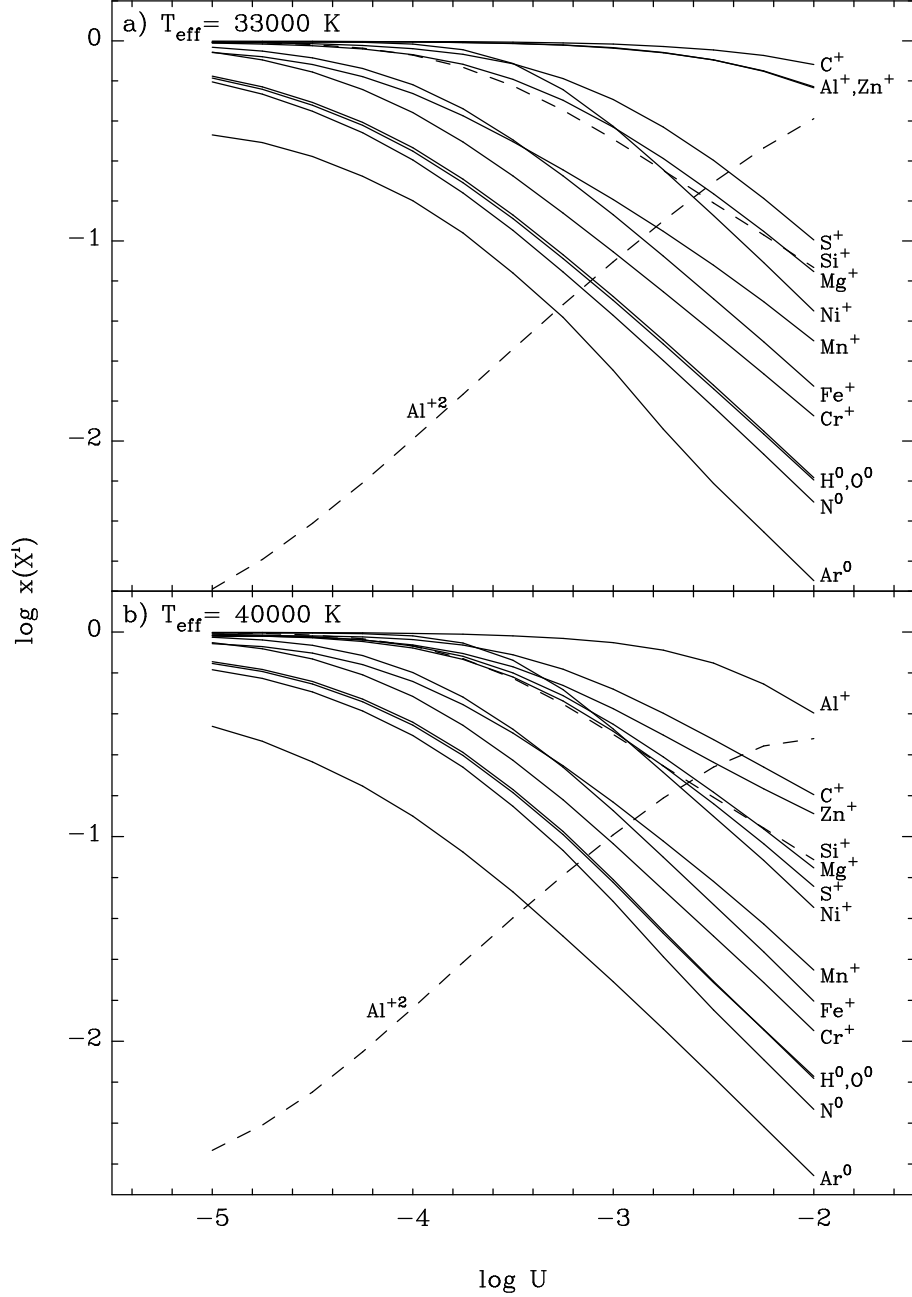


Fig. 1.— Ionic fractions of elements along the line of sight $x(X^i)$ as a function of ionization parameter U for the closed plane-parallel H II region models ionized by stellar radiation with (a) $T_{\text{eff}} = 33000 \text{ K}$ and (b) 40000 K . The curves for Al^{+2} and Si^+ are shown by dashed lines.

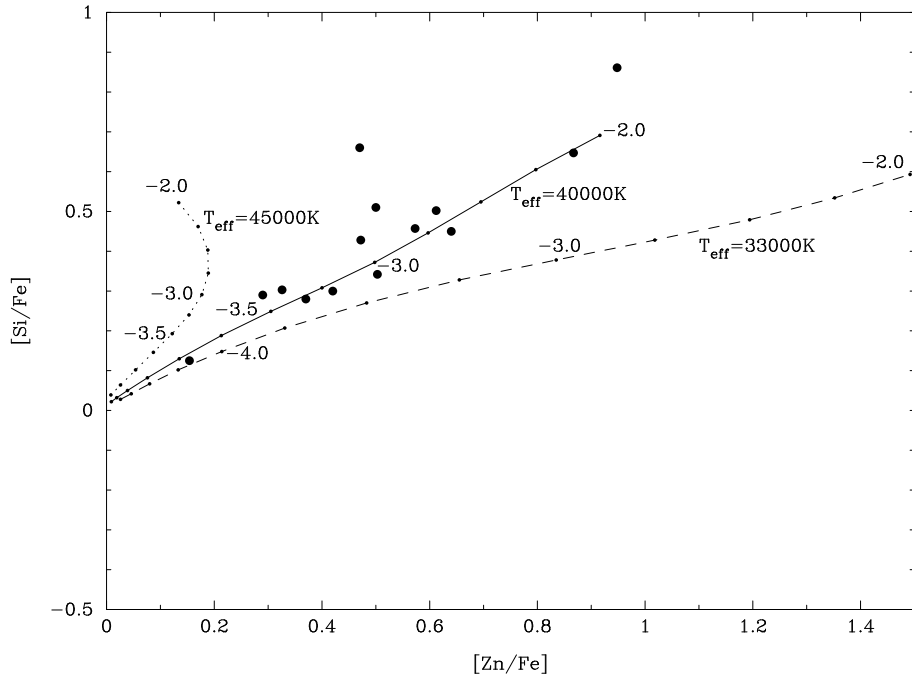


Fig. 2.— The $[\text{Si}/\text{Fe}]$ vs $[\text{Zn}/\text{Fe}]$ relation. The filled circles are observational points from Prochaska & Wolfe (1999). Dashed, solid and dotted lines connect theoretical points $[x(\text{Si}^+)/x(\text{Fe}^+), x(\text{Zn}^+)/x(\text{Fe}^+)]$ in models with $Z = 0.1 Z_{\odot}$ for varying values of the ionization parameter U (in steps of 0.25 dex) marked by numbers in log scale respectively, and for three values of the effective temperature $T_{\text{eff}} = 33000$ K, 40000 K and 45000 K.

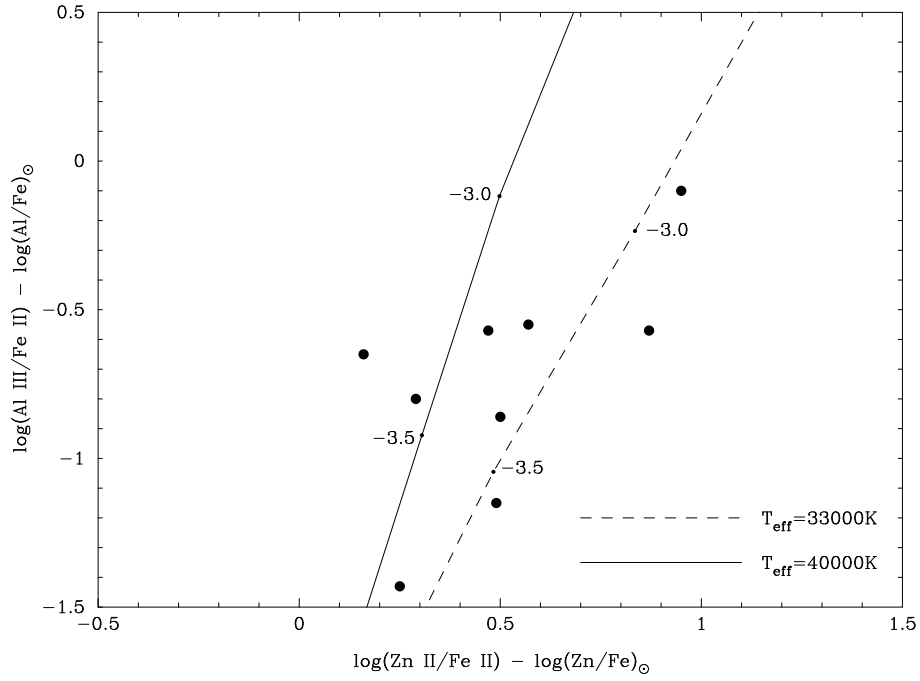


Fig. 3.— The [Al III/Fe II] vs [Zn II/Fe II] relation. The filled circles are observational points from Prochaska & Wolfe (1999) and Lu et al. (1996a). Dashed and solid lines connect theoretical points $[x(\text{Al}^{+2})/x(\text{Fe}^+)]$, $[x(\text{Zn}^+)/x(\text{Fe}^+)]$ in models with $Z = 0.1 Z_\odot$ for varying values of the ionization parameter U marked by numbers in log scale respectively, and for two values of the effective temperature $T_{\text{eff}} = 33000 \text{ K}$ and 40000 K .

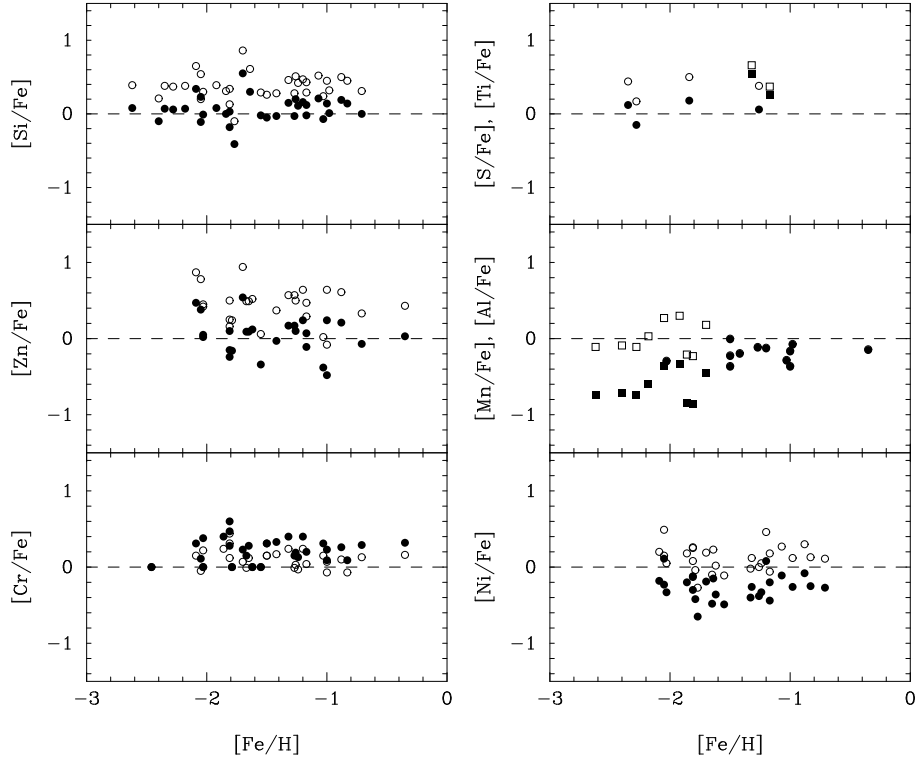


Fig. 4.— Heavy element abundance ratios for DLAs from Lu et al. (1996), Prochaska & Wolfe (1999) and Pettini et al. (1999). Open symbols are observed abundance ratios while filled symbols are abundance ratios corrected for ionization effects. Squares are data for $[\text{Ti}/\text{Fe}]$ and $[\text{Al}/\text{Fe}]$ while circles are for other heavy element abundance ratios. The ionization-bounded plane-parallel model with ionization parameter $\log U = -3.25$ and stellar radiation temperature $T_{\text{eff}} = 40000$ K is adopted.

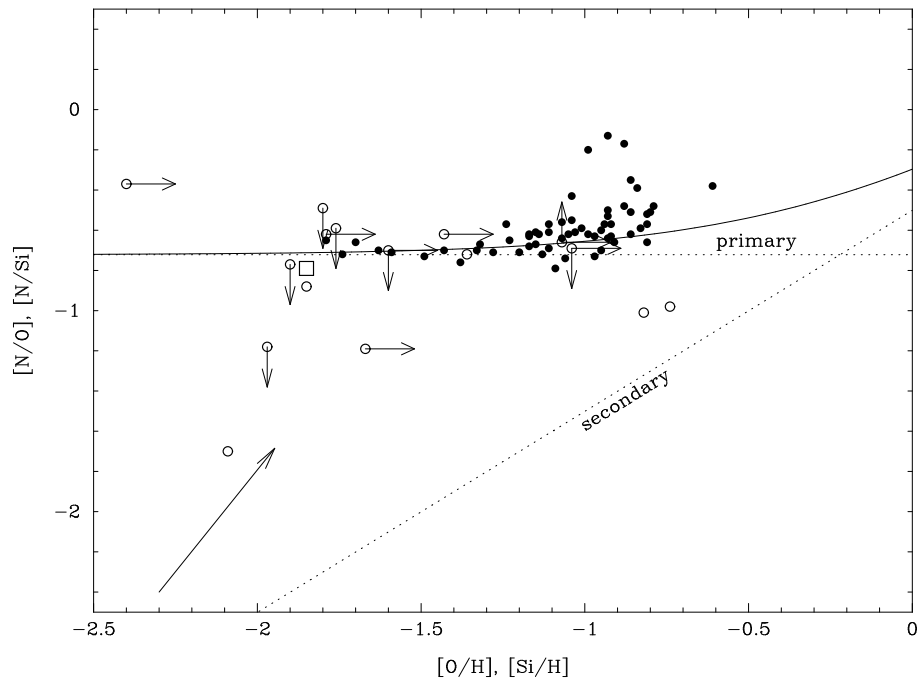


Fig. 5.— $[N/O]$, $[N/Si]$ vs $[O/H]$, $[Si/H]$ diagram. Open circles are $[N/Si]$ vs $[Si/H]$ for DLAs from Lu et al. (1998) and Outram et al. (1999), open square are $[N/O]$ vs $[O/H]$ for DLA from Molaro et al. (2000), filled circles are $[N/O]$ vs $[O/H]$ for blue compact dwarf galaxies from Izotov & Thuan (1999). Dotted lines are diagrams for primary and secondary productions of nitrogen, while solid line is dependence $[N/O]$ vs $[O/H]$ when both primary and secondary productions of nitrogen are taken into account. Solid line with arrow in the lower left corner shows the value and direction of abundance ratio correction for the ionization-bounded plane-parallel model with ionization parameter $\log U = -3.25$ and stellar radiation temperature $T_{\text{eff}} = 40000$ K.